Mechanisms of Action of Bactericidal/Permeability-Increasing Protein BPI on Reconstituted Outer Membranes of Gram-Negative Bacteria†

Andre Wiese,‡ Klaus Brandenburg,‡ Stephen F. Carroll,§ Ernst Th. Rietschel,‡ and Ulrich Seydel*,‡

Department of Immunochemistry and Biochemical Microbiology, Center for Medicine and Biosciences, Research Center Borstel, Parkallee 10, D-23845 Borstel, Germany, and XOMA Corporation, 2910 Seventh Street, Berkeley, California 94710

Received January 24, 1997; Revised Manuscript Received June 9, 1997⊗

ABSTRACT: The mechanisms of interaction of the recombinant N-terminal portion of bactericidal/permeability-increasing protein, $rBPI_{21}$, with various planar asymmetric and symmetric bilayer membranes, including the lipid matrix of the outer membrane of Gram-negative bacteria, were investigated via electrical measurements. For the lipopolysaccharide (LPS) leaflet of the outer membrane, isolated deep rough mutant LPS of *Escherichia coli* strain F515 (F515 LPS) and *Proteus mirabilis* strain R45 (R45 LPS) were used. The addition of $rBPI_{21}$ to the LPS side of asymmetric LPS/phospholipid membranes, as well as to black lipid membranes made from dioleoylphosphatidylglycerol (DOPG), led to membrane rupture. The innermembrane potential difference resulted in a slight increase from 0 to 5 mV for symmetric DOPG membranes but changed for asymmetric F515 LPS/PL membranes from −36 to +8 mV and for R45 LPS/PL membranes from −37 to −5 mV following the addition of $rBPI_{21}$. In all cases, the addition of $rBPI_{21}$ led to an increase in membrane current. The effect of $rBPI_{21}$ on the innermembrane potential difference of LPS/PL membranes was significantly reduced in the presence of 40 mM $MgCl_2$ (shift from −36 to −31 mV for F515 LPS). On the basis of these results and from our studies on the interaction of $rBPI_{21}$ with lipid monolayers and aggregates [Wiese, A., et al. (1997) *Biochemistry 36*, 10301−10310], a model is discussed explaining how the observed membrane rupture, increase of membrane current, and change of transmembrane potential as induced by $rBPI_{21}$ may contribute to bacterial dysfunction.

The cell envelope of Gram-negative bacteria consists of the cytoplasmic membrane, the peptidoglycan layer, and an additional barrier, the outer membrane, which is strictly asymmetric with respect to its lipid composition. Whereas the inner leaflet of this membrane contains only phospholipids, the outer leaflet is made up mainly from lipopolysaccharides (LPS),[1] which consist of an oligo- or polysaccharide moiety and a covalently linked lipid component, termed lipid A, anchoring the LPS in the outer membrane (Rietschel et al., 1996). LPS has been shown to play a major role in pathophysiology of severe Gram-negative sepsis and, thus, represents a target for antisepsis strategies. Its association with the cell surface renders LPS a particularly interesting target as it may serve as a receptor for antibacterial drugs.

A naturally occurring protein possessing the capacity to bind to bacteria-associated LPS resulting in reduction of bacterial viability and to neutralize LPS is bactericidal/permeability-increasing protein (BPI), an antibacterial polypeptide of polymorphonuclear neutrophils (PMN) capable of killing bacteria by oxygen-independent mechanisms. BPI is located in the azurophilic granules of neutrophils (Weiss & Olsson, 1987) and is an approximately 55 kDa cationic protein with a selectivity toward Gram-negative bacteria (Weiss et al., 1978; Elsbach et al., 1979), most likely due to its strong affinity for LPS (Gazzano-Santoro et al., 1992, 1995). Beside being bactericidal (Weiss et al., 1975, 1978, 1984; Elsbach & Weiss, 1993; Capodici et al., 1994), BPI also neutralizes the cytotoxic effects of LPS (Ooi et al., 1991; Elsbach & Weiss, 1993). Most of the antibacterial and LPS-binding activity of holo-BPI is found in 20−25 kDa N-terminal fragments of the protein (Ooi et al., 1987, 1991; Capodici et al., 1994; Gazzano-Santoro et al., 1992; Horwitz et al., 1996). N-Terminal fragments of BPI also inhibit LPS-induced E-selectin expression and reduce NF-κB activation in LPS-stimulated endothelial cells (Huang et al., 1995). Furthermore, $rBPI_{21}$, representing a recombinant 21 kDa protein and corresponding to amino acids 1−193 of N-terminal human BPI (with the exception that a cysteine is replaced by an alanine at position 132) is bactericidal and binds to and neutralizes endotoxin (Horwitz et al., 1996). Therefore, experiments in animals (Kartalija et al., 1995; Koyama et al., 1995; Lechner et al., 1995; Hansbrough et al., 1996) and human trials (de Winter et al., 1995; Kirsch et al., 1997) with N-terminal fragments of BPI have been performed.

† This work was financially supported by the German Federal Minister of Education, Science, Research and Technology (BMBF Grant 01 KI 9471), the Deutsche Forschungsgemeinschaft (SFB 367, Projects B2 and B8, and SFB 470, Projects B4 and B5), and the Fonds der Chemischen Industrie (to E.Th.R.).

* To whom correspondence should be addressed.

‡ Research Center Borstel.

§ XOMA Corporation.

⊗ Abstract published in *Advance ACS Abstracts,* August 1, 1997.

[1] Abbreviations: LPS, lipopolysaccharide; F515 LPS, lipopolysaccharide of the *Escherichia coli* Re mutant strain F515; R45 LPS, lipopolysaccharide of the *Proteus mirabilis* Re mutant strain R45; BPI, bactericidal/permeability-increasing protein; $rBPI_{23}$, 23 kDa N-terminal fragment of bactericidal/permeability-increasing protein; $rBPI_{21}$, 21 kDa N-terminal fragment of bactericidal/permeability-increasing protein; PMN, polymorphonuclear neutrophils; PMB, polymyxin B; PMBN, polymyxin B nonapeptide; PE, phosphatidylethanolamine; PG, phosphatidylglycerol; DPG, diphosphatidylglycerol; PL, lipid mixture composed of phosphatidylethanolamine, phosphatidylglycerol, and diphosphatidylglycerol in molar ratios of 81:17:2; DOPG, dioleoylphosphatidyglycerol; BLM, black lipid membrane; U_D, dipole potential; U_B, Born potential.

S0006-2960(97)00177-3 CCC: $14.00

In a preceding study [Wiese et al., 1997 (preceding paper in this issue)], we showed that $rBPI_{21}$ binds to and intercalates into monolayers and aggregates containing negatively charged lipids. Here, we report on studies aiming at an understanding of the consequences of these interactions on the function of the bacterial outer membrane. As a model, we have studied the action of $rBPI_{21}$ on the outer membrane reconstituted as an asymmetric planar bilayer, consisting of LPS on one side and of a phospholipid mixture (PL) on the other, the PL mixture resembling the composition of the inner leaflet of the bacterial outer membrane (Seydel et al., 1989). This reconstituted system allowed us to obtain information on $rBPI_{21}$-induced changes in the electrical properties of the lipid bilayer such as membrane potential (determined from current/voltage curves of K^+-carrier-doped membranes) and membrane conductivity (from measurements of membrane current). To acquire information on the lipid specificity of $rBPI_{21}$, we have performed similar measurements with symmetric (black lipid) membranes made from dioleoylphosphatidylglycerol (DOPG).

The results of the present study of the action of $rBPI_{21}$ on the reconstituted outer membrane of Gram-negative bacteria, in combination with known data about the interaction mechanism of $rBPI_{21}$ with the lipid matrix (Wiese et al., 1997), allowed us to develop the following model. $rBPI_{21}$, after binding to the negatively charged lipid surface, inserts into the lipid matrix, an event that causes rigidification of the acyl chains of the LPS layer and its destabilization, eventually provoking membrane rupture. The binding and insertion of $rBPI_{21}$ results in significant changes of the membrane current, influencing membrane permeability for hydrophobic molecules, and of the transmembrane potential, which may influence channel gating, subsequently causing membrane dysfunction.

MATERIALS AND METHODS

Materials

Lipids and Other Chemicals. LPS of the deep rough (Re) mutant of *Escherichia coli* strain F515 (F515 LPS) was used in experiments with asymmetric F515 LPS/PL membranes. Some experiments were performed with R45 LPS, which was isolated from the deep rough mutant of *Proteus mirabilis* strain R45. LPS was extracted by the phenol/chloroform/petroleum ether method (Galanos et al., 1969), purified, lyophilized, and dialyzed. Dialysis guaranteed that the LPS samples contained less than 1 divalent cation per 100 LPS molecules as proven by atomic absorption spectroscopy.

Phosphatidylethanolamine (PE) from *E. coli*, phosphatidylglycerol (PG) from egg yolk (sodium salt), diphosphatidylglycerol (DPG) from bovine heart (disodium salt), and dioleoylphosphatidyglycerol (DOPG) were purchased from Avanti Polar Lipids (Alabaster, AL) and used without further purification. Natural phospholipids for the preparation of Montal−Mueller membranes were dissolved (2.5 mg/mL) in chloroform, and LPS was dissolved (2.5 mg/mL) in chloroform/methanol (10:1 v/v).

The K^+ carrier nonactin was obtained from Sigma (St. Louis, MO).

Proteins. $rBPI_{21}$, a recombinant N-terminal fragment of human BPI, was produced and purified as described (Horwitz et al., 1996) and was obtained as a sterile, nonpyrogenic solution at a concentration of 3 mg/mL in citrate-buffered saline (150 mM NaCl and 5 mM sodium citrate, pH 5) without detergents or stabilizers. The $rBPI_{21}$ samples were aliquoted, frozen in liquid nitrogen, and stored at −70 °C. Before use, the samples were thawed, kept at 4 °C, and used within 1 week. The bactericidal activity of $rBPI_{21}$ was tested prior to use against *E. coli* J5 as described by Capodici et al. (1994).

The nonapeptide of polymyxin B (PMBN) was obtained from Boehringer (Mannheim, Germany).

Preparation of Planar Bilayers and Electrical Measurements

Lipid Bilayers According to the Montal−Mueller Method. Planar bilayers according to the Montal−Mueller technique (Montal & Mueller, 1972) were prepared as described before (Seydel et al., 1989). The apparatus for membrane formation consisted of two Teflon compartments of 1.5 mL volume each, which were separated by a Teflon septum (12.5 μm thick) having a small aperture (typically 110 μm diameter). Prior to membrane formation, the septum was treated with a hexane/hexadecane mixture (20:1 v/v). Membranes were finally formed by apposing the two identically or differently composed lipid monolayers, each spread on aqueous bathing solutions, over the aperture. For the reconstitution of the outer leaflet of the lipid matrix of the outer membrane, Re LPS was used. The inner leaflet of the outer membrane was reconstituted from a lipid mixture (PL) composed of PE, PG, and DPG in a molar ratio of 81:17:2. This particular mixture corresponds to that determined for Gram-negative bacteria, e.g., *Salmonella typhimurium* (Osborn et al., 1972). For electrical measurements, planar membranes were voltage-clamped via a pair of Ag/AgCl electrodes (Type IVM E255, Zak GmbH, Simbach, Germany) that were connected to the headstage of a BLM 120 bilayer membrane amplifier (Biologic, Claix, France) with a feedback resistor of 1 GΩ (the side opposite to protein addition was grounded). Membrane current and holding voltage were stored on a DAT tape recorder (DTR 1200, Biologic). The stored signals were sent to the microcomputer system filtered by a 4-pole low-pass Bessel filter (Ithaco Scientific Instruments, Ithaca, NY), the corner frequency of which was adjusted to 10 Hz (−3 dB) and digitized at a sampling rate of 10 Hz with a PCI 20089W-1 analog input board (Intelligent Instrumentation). Current was positive when cation flux was directed toward the grounded compartment.

Black Lipid Membranes. Symmetric membranes were prepared according to the method of Mueller and Rudin (Mueller et al., 1963), because this technique yielded a better stability as compared to membranes prepared by the Montal−Mueller technique. For the formation of so-called black lipid membranes (BLM), a solution of DOPG (10 mg/mL) in *n*-decane was spread over the aperture (typically 520 μm diameter) which connects the inner volume (0.8 mL) of a perspex compartment with the chamber (4.2 mL) of the surrounding Teflon block (DOPG was used instead of PG because of its solubility in *n*-decane). For the measurement of membrane current, a bilayer headstage with 1 GΩ feedback resistor, Type HAMK2TC, was connected to a bilayer power supply, Type BPS06/01 (R. A. P. Montgomery, London, U.K.). The thinning process of the membrane was monitored via the measurement of the membrane capacitance

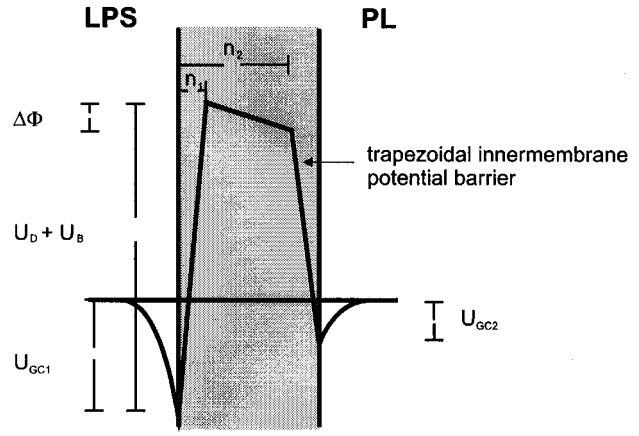

FIGURE 1: Schematic representation of the intrinsic membrane potential profile for F515 LPS/PL membranes [adopted from Schoch et al. (1979)]. Negative surface charges induce the Gouy-Chapman potential U_{GC}. The trapezoidal innermembrane potential barrier is caused by the dipole potential (U_D) and the self energy (Born potential, U_B). $\Delta\Phi$, innermembrane potential difference; n_1 and n_2, positions of the corners of the trapezoidal potential barrier.

applying the voltage-induced capacitance relaxation method (Benz & Janko, 1976). For this purpose, the headstage was modified in a way that the clamp voltage could be switched to the output of a function generator (Voltcraft FG-506, Conrad Electronic, Hirschau, Germany). The side opposite to protein addition was grounded. The output signals were filtered with an 8-pole Butterworth low-pass filter type 901 (Frequency Devices, Haverhill, MA) at a corner frequency of 20 Hz. If necessary, the signals could further be amplified by a factor of 10. Data storage and digitization were done as described for the Montal−Mueller membranes.

Membrane Potential

The intrinsic membrane potential is composed of the surface potential and the innermembrane potential. The sum of the intrinsic membrane potential and a potential resulting from an externally applied clamp voltage (or from a transmembrane ion gradient) results in the transmembrane potential [Figure 1; adopted from Schoch et al. (1979) for LPS/PL membranes].

The surface potential is provoked by fixed charges on the membrane surface. The innermembrane potential arises from the dipole potential (U_D), which is created by dipole moments within the lipid matrix and the interface region of the bilayer and the adsorbed water molecules, and from the Born self-energy (Born potential, U_B) of a charge in the low-dielectric medium of the membrane [Schoch et al., 1979; for review on membrane electrostatics see also Cevc (1990)].

Lipid asymmetry may provoke a potential difference between the two surfaces of the bilayer membrane. An asymmetric potential profile has been observed in membranes with an asymmetric distribution of the surface charge densities on the opposing monolayers (Hall & Latorre, 1976), in membranes with a symmetric distribution of the charge densities but with an asymmetry with respect to the headgroup conformations of the two leaflets (Latorre & Hall, 1976), and for symmetric membranes with asymmetry of the subphases (Schoch et al., 1979). An extreme asymmetry in charge densities as well as in headgroup conformations occurs for asymmetric LPS/PL bilayers. At neutral pH, of the phospholipids only the phosphatidylglycerol molecule carries one negative charge, whereas each F515 LPS molecule carries four negative charges. The resulting surface charge densities are -0.52 As/m^2 ($-3.25e_0$/nm^2) for F515 LPS and -0.05 As/m^2 ($-0.31e_0$/nm^2) for the PL mixture, respectively, since the molecular cross-section of an F515 LPS molecule is 1.23 nm^2 and that of a diacylphospholipid is 0.55 nm^2 (determined from monolayer isotherms with a film balance). In the R45 LPS molecule, the 4′-phosphate and the first Kdo are nonstoichiometrically substituted with 4-amino-4-deoxy-L-arabinopyranose (Vinogradov et al., 1994). As could be shown by MALDI mass spectroscopy (data not shown), total substitution is approximately 50%, resulting in about 3 negative charges/molecule and a surface charge density of -0.38 As/m^2 corresponding to $-2.36e_0$/nm^2 (molecular area of 1.27 nm^2). From these surface charges, the surface potential can be calculated according to the Gouy equation (McLaughlin, 1989):

$$U_{GC} = \frac{2kT}{Ze_0} a\sinh \frac{\sigma}{(8\epsilon\epsilon_0 kTN_A c)^{1/2}} \qquad (1)$$

where k is the Boltzmann constant, T is the absolute temperature, ϵ is the relative dielectric number of the subphase, ϵ_0 is the dielectric constant, e_0 is the elementary charge, Z is the valence of the counterions, c is the concentration of the subphase (here, the ionic strength of the bathing solutions), N_A is Avogadro's number and σ is the surface charge density (all in SI units). The calculated values give only a crude estimation because the binding effects, especially of the divalent Mg^{2+}, ions, were neglected.

To study the influence of $rBPI_{21}$ on the intrinsic membrane potential, we calculated the innermembrane potential difference $\Delta\Phi$ from current/voltage (I/U) characteristics of carrier-doped bilayer membranes.

Innermembrane potential profiles were derived from I/U curves obtained from K^+-carrier-doped bilayers. For these studies, membranes according to the Montal−Mueller technique and BLM were prepared as described above in a bathing solution consisting of 100 mM KCl and 2 mM $MgCl_2$ (for membrane stabilization) or 50 mM KCl, respectively, buffered with 5 mM HEPES at pH 7. The K^+ carrier nonactin was added to both compartments before membrane preparation at a final concentration of 5×10^{-7} M in the case of Montal−Mueller membranes and 5×10^{-8} M in the case of BLM.

The electric current through carrier-doped membranes provides two different types of information. From changes in the current upon $rBPI_{21}$ addition at a fixed voltage, changes in the height of the potential barrier within the membrane can be calculated according to

$$\Delta\psi = -\frac{RT}{F} \ln \frac{I}{I_0} \qquad (2)$$

where I_0 is the current before and I is the current after the addition of $rBPI_{21}$ (McLaughlin, 1977). The potential profile across the various bilayers before and after addition of $rBPI_{21}$ to the cis compartment was probed via the registration of I/U characteristics. For this purpose, the applied voltage (cis compartment grounded) could be varied in 1 mV steps by a built-in power supply or continuously via an external control voltage. The latter was connected to the membrane amplifier from an analog output card PCI 20093-W (Intelligent

Instrumentation, Leinfelden-Echterdingen, Germany) plugged into an AT-compatible microcomputer system. The evaluation of the *I*/*U* curves was done according to procedures described previously (Seydel et al., 1992). Briefly, the current I as a function of the voltage U applied with the voltage clamp is obtained from

$$I_m = K\frac{[\Delta\Phi + (n_2 - n_1)U]}{(n_2 - n_1)}\frac{e^{aU} - 1}{e^{a(\Delta\Phi + n_2U)} - e^{an_1U}} \quad (3)$$

where $a = (Ze_0)/(kT)$, K is a constant for each membrane (depending, among other things, on its area and thickness), n_1 and n_2 are the relative distances of the edges of the potential walls for the two leaflets to the membrane surface on the cis side, and $\Delta\Phi$ is the potential difference between these edges (Schoch et al., 1979). The three parameters describe the shape of the trapezoidal energy barrier and were determined from the experimental curves by computer fitting of eq 3.

RESULTS

Influence on Membrane Conductance. Membrane conductance is a measure for the integrity of the lipid bilayer. An intact, undisturbed bilayer has a negligible electrical conductivity. Static or transient pores or lesions cause a transient or permanent increase of conductivity. Thus, the measurement of membrane conductivity of differently composed lipid bilayers should yield information on any perturbing effects of $rBPI_{21}$ and, with that, on its membrane activity.

For asymmetric F515 LPS/PL membranes and at a clamp voltage of +20 mV, the addition of 500 nM $rBPI_{21}$ to the F515 LPS side led to a relatively small increase in membrane current and to a noisy current signal. Upon switching the clamp voltage between negative and positive polarity with increasing absolute values, the membrane current increased proportionally. At positive clamp voltages the membrane broke at +50 mV (Figure 2); at negative clamp voltages the absolute value of the breakdown voltage was significantly higher (≤ -80 mV). At $rBPI_{21}$ concentrations > 1 μM, the membranes broke immediately after protein addition even at zero clamp voltage.

For R45 LPS/PL membranes, the addition of the same amount of $rBPI_{21}$ to the R45 LPS side did not induce any conductance changes at clamp voltages below +50 mV (data not shown).

For BLMs made from DOPG, a current proportional to the clamp voltage was observed prior to the addition of the protein (Figure 3). The addition of 60 nM $rBPI_{21}$ caused single current fluctuations above a clamp voltage of +40 mV (Figure 3B). The current increased with increasing clamp voltage, and the single current fluctuations were followed by a macroscopic current increase, finally leading to membrane rupture. Upon changing the polarity, these effects were observed only at clamp voltages ≤ -80 mV. Recordings at higher sample frequencies (1 kHz instead of 10 Hz) allowed the calculation of the single fluctuation conductivity, which was in the range of 0.4−0.8 nS for the DOPG membranes and did not significantly depend on the applied clamp voltage. The mean lifetime of the conductance fluctuations was about 2 ms. From the mean single fluctuation conductivity and the specific conductivity of the subphase (14 mS/cm for 150 mM NaCl at room temperature),

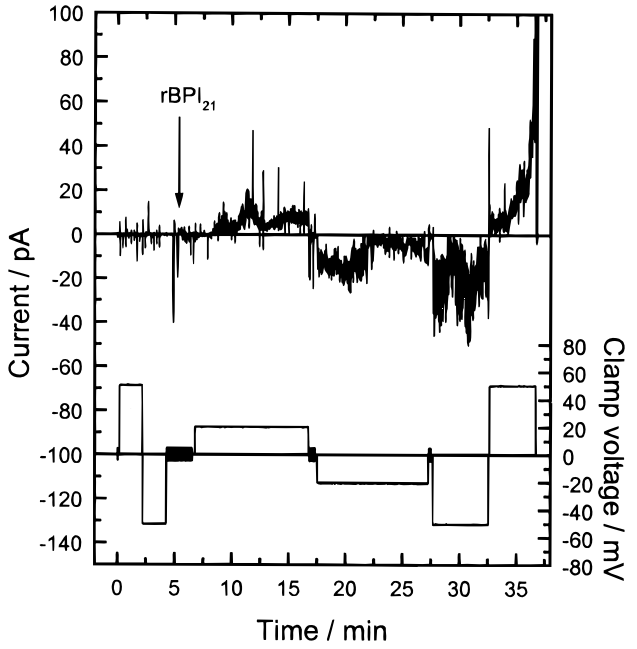

FIGURE 2: Membrane current (upper trace) and clamp voltage (lower trace) for an asymmetric F515 LPS/PL membrane. Addition of 500 nM $rBPI_{21}$ to the LPS side is indicated by arrow (PL-side grounded). Bathing solution: 0.15 M NaCl, 5 mM HEPES-buffered at pH 7, $T = 37$ °C.

the lesion diameter was calculated to be 1.5−2.1 nm assuming a cylindrical geometry of the lesion and a membrane thickness of 6 nm. Evaluation of the conductivity of single fluctuations [based on the quotient of the current variance and the mean current according to Neher and Stevens (1977) and assuming that the macroscopic current results from the superposition of independent fluctuations with very small probabilities] gave a value of about 3 pA independent of the applied clamp voltage. From the mean membrane current, a conductivity of the single lesion between 0.02 and 0.11 nS could be derived. At higher $rBPI_{21}$ concentrations (180 nM), current increases could be observed even at zero clamp voltage. Under these conditions, a sudden membrane rupture often occurred, and at still higher protein concentrations (>1 μM) the membranes broke in all experiments immediately (data not shown).

To determine whether divalent cations protect the membrane against the action of $rBPI_{21}$, measurements with a bathing solution containing 40 mM $MgCl_2$ were performed. In these experiments, even at $rBPI_{21}$ concentrations of 350 nM and clamp voltages up to $\pm$100 mV no $rBPI_{21}$ effects could be observed. However, after further addition of $rBPI_{21}$ (final concentration 500 nM) the membranes broke down at +100 mV, whereas they withstood negative voltages of −100 mV (data not shown).

Membrane Potential. The determination of the intrinsic membrane potential—a combination of surface potential, dipole potential, and innermembrane potential difference—provides information on the interaction of externally applied compounds because their interaction with the lipid bilayer may induce changes in the intrinsic membrane potential profile, in particular when these substances carry electric charges. The induced changes in the transmembrane potential may also influence the function of membrane proteins and thus contribute to the impairment of bacterial functions. To acquire information on changes in the inner-

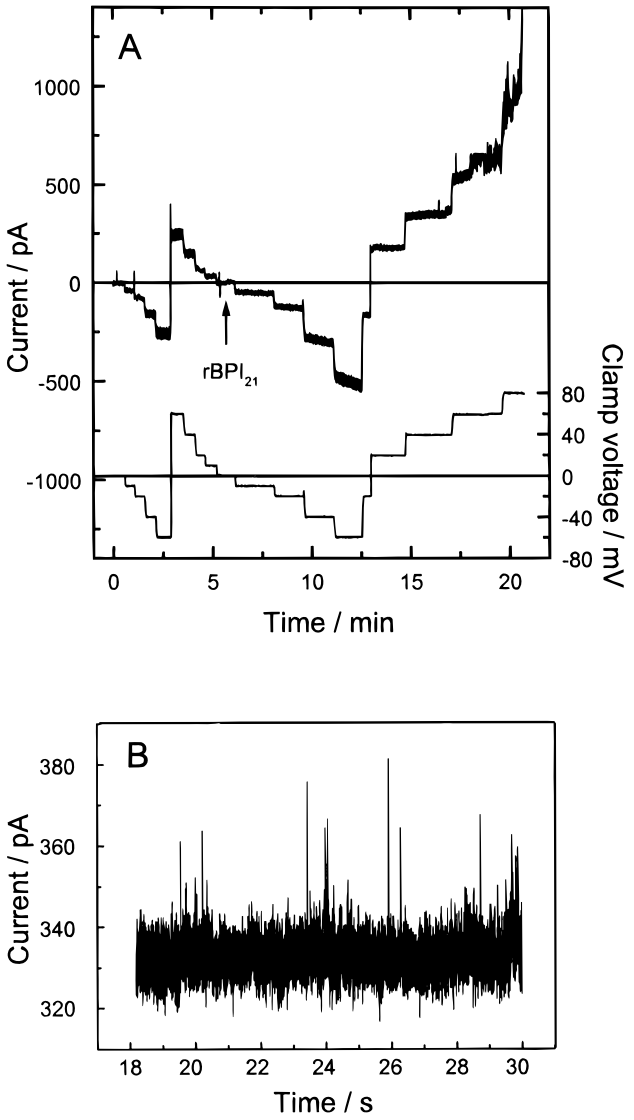

FIGURE 3: (A) Membrane current (upper trace) and clamp voltage (lower trace) for a painted membrane of DOPG. Addition of 60 nM $rBPI_{21}$ to the cis side is indicated by arrow (trans-side grounded). (B) Single current fluctuations at a clamp voltage of +40 mV; sampling rate 1 kHz. Bathing solution: 0.15 M NaCl, 5 mM HEPES-buffered at pH 7, $T = 20$ °C.

membrane potential, we recorded *I*/*U* curves of K^+-carrier-doped planar membranes in the absence and presence of $rBPI_{21}$, PMBN, and Mg^{2+}.

The addition of $rBPI_{21}$ (final concentration of 300 nM) to the LPS side of an asymmetric F515 LPS/PL or R45 LPS/PL membrane doped with nonactin led to an increase in membrane conductivity by a factor of 3−5 without any induction of current fluctuations. In Figure 4, only the results for the former system are depicted. In the case of nonactin-doped BLMs prepared from DOPG, the addition of 100 nM $rBPI_{21}$ to one side of the membrane only increased the conductivity by a factor of ≤2 (data not shown). It should be noted that $rBPI_{21}$ concentrations used for the Montal−Mueller membranes and for BLMs cannot be compared quantitatively because of the different preparation techniques and the larger membrane area of BLMs. Furthermore, the concentration of $rBPI_{21}$ at the membrane surface might be different from that in the bathing solution due to accumulation of the polycationic $rBPI_{21}$ at the negatively charged membrane surface. According to eq 1, the height of the innermembrane potential barrier is decreased by a value between 29 and 43 mV in the case of LPS/PL membranes and by less than 17 mV in the case of DOPG BLMs.

The measured *I*/*U* curves and the respective fits (according to eq 3) for asymmetric F515 LPS/PL membranes before (Figure 4A) and after (Figure 4B) the addition of 300 nM $rBPI_{21}$ or PMBN clearly show that the asymmetry of the characteristic is reversed and the potential difference $\Delta\Phi$ rises from −36 mV before to +8 mV after addition of $rBPI_{21}$. The respective shift in $\Delta\Phi$ for R45 LPS/PL membranes was from −37 to −5 mV (data not shown). The addition of the same concentration of PMBN to the LPS side of F515 LPS/PL membranes did not significantly alter membrane conductivity and, in contrast to $rBPI_{21}$, changed the potential difference from −36 to −47 mV.

To study the role of Mg^{2+} in the interaction of $rBPI_{21}$ with the outer membrane, we have determined the influence of Mg^{2+} alone and in the absence and presence of $rBPI_{21}$ on the innermembrane potential of nonactin-doped F515 LPS/PL-membranes. $MgCl_2$ (40 mM) in the bathing solution reduced the membrane current by a factor of ≤5 and increased the asymmetry of the *I*/*U* curves from −36 to −59 mV (Figure 5). In the absence of $MgCl_2$, $rBPI_{21}$ led to an increase of membrane current and shift of $\Delta\Phi$ from −36 to −31 mV (Figure 5B). The change in the height of the potential barrier was calculated to be ≤42 mV. In most cases, the fits for the *I*/*U* curves were ideal; i.e., they superimposed the measured data completely. The values for the parameters n_1 and n_2 were 0.22 and 0.78, respectively. In the case of symmetric DOPG BLMs, only a slight increase of $\Delta\Phi$ from 0 to approximately 5 mV for $rBPI_{21}$ concentrations from 0 to 140 nM could be observed (data not shown).

In combination with the known changes of the surface potential, which were derived from ζ-potential measurements (Wiese et al., 1997), the data obtained from the carrier measurements allow us to make estimations of the membrane potential profiles. In Figure 6, the potential profiles are depicted for F515 LPS/PL membranes in bathing solutions in the absence and presence of 40 mM $MgCl_2$ and in the absence and presence of $rBPI_{21}$ or PMBN on the LPS side of the membrane. The data of Figure 6B once more show that $rBPI_{21}$ led to an increase of $\Delta\Phi$, whereas PMBN and Mg^{2+} led to a decrease, and that $rBPI_{21}$ did not provoke an additional change in $\Delta\Phi$ in the presence of 40 mM $MgCl_2$. The changes in $\Delta\Phi$ induced by PMBN, but not by $rBPI_{21}$, corresponded to the changes in the ζ-potential. The height of the potential barrier (refered to the midpoint of the slope of the innermembrane potential) was not changed by PMBN but was increased by Mg^{2+} and decreased by $rBPI_{21}$.

DISCUSSION

The antibacterial action of BPI and its bioactive N-terminal fragments is promoted by their binding to the outer membrane, thus triggering immediate alterations of the outer envelope, e.g., enhancement of its permeability toward hydrophobic antibiotics like actinomycin D (Weiss et al., 1978) and inhibition of the growth of susceptible microbes. The sublethal effects of this initial phase are reversed by addition of high concentrations of $MgCl_2$ (≥40 mM) or 0.1% bovine serum albumin to the growth medium (Weiss et al., 1978; Mannion et al., 1990). This reversible phase is apparently followed by an irreversible phase, which may be

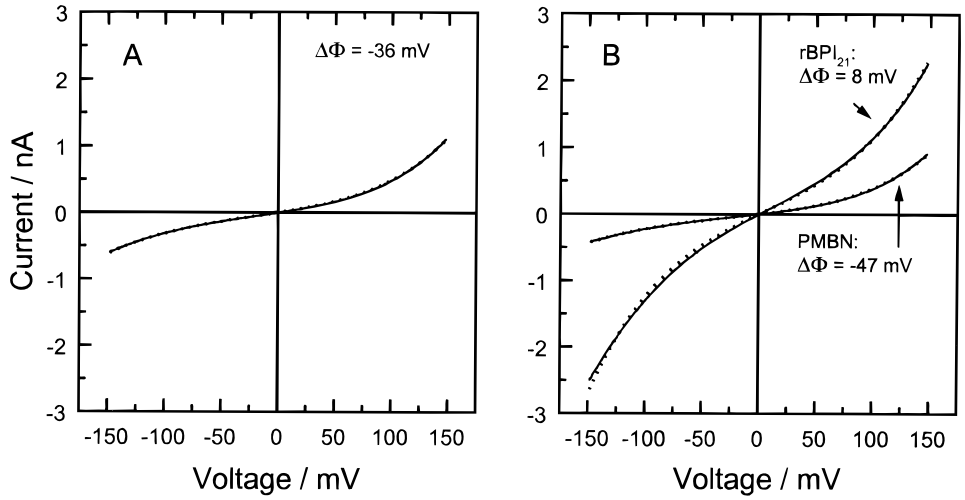

FIGURE 4: *I*/*U* curves and derived innermembrane potential differences of nonactin-doped asymmetric F515 LPS/PL membranes before (A) and after (B) the addition of $rBPI_{21}$ and PMBN, respectively, to the LPS side. Bathing solution: 0.1 M KCl and 2 mM $MgCl_2$, 5 mM HEPES-buffered at pH 7, $T = 37$ °C. The fits (dotted lines) were calculated according to eq 3.

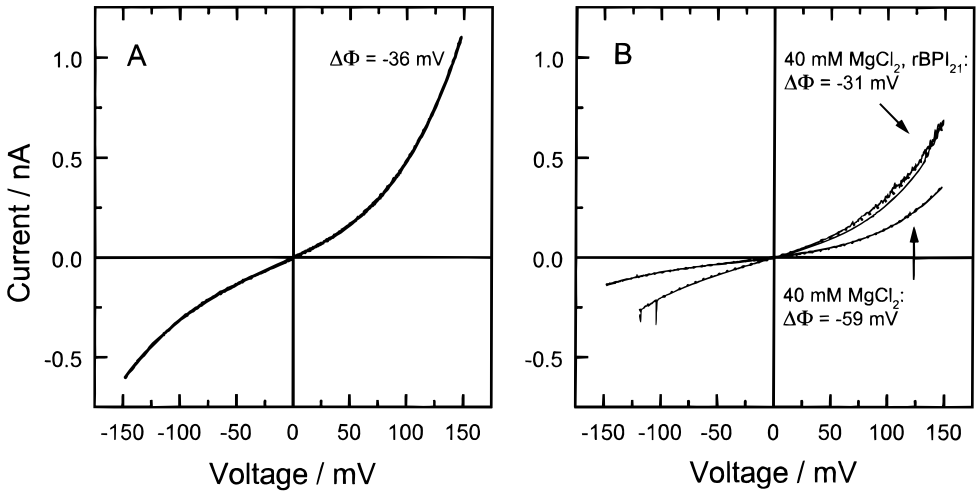

FIGURE 5: *I*/*U* curves and derived innermembrane potential differences of nonactin-doped asymmetric F515 LPS/PL membranes without (A) and with (B) additional 38 mM $MgCl_2$ in the absence and presence of $rBPI_{21}$ on the LPS side. Bathing solution: 0.1 M KCl and 2 mM $MgCl_2$, 5 mM HEPES-buffered at pH 7, $T = 37$ °C. The fits (dotted lines) were calculated according to eq 3.

due to alterations of the cytoplasmic membrane (In't Veld et al., 1988). For an understanding of these BPI effects we recently investigated the interaction of $rBPI_{21}$ with lipid monolayers and aggregates [Wiese et al., 1997 (preceding paper in this issue)]. It was shown that $rBPI_{21}$ binds to and incorporates into monolayers and aggregates of negatively charged lipids. Due to this incorporation the negative surface potential and the fluidity of the hydrocarbon moieties were reduced. On the basis of the results of the present study, we now present a model that may explain the $rBPI_{21}$-induced bacterial dysfunction on the basis of membrane rupture, increase of membrane current, and change of transmembrane potential.

In this paper, we studied the interaction of $rBPI_{21}$ with various model membrane systems including an asymmetric bilayer composed of LPS on one side and a phospholipid mixture on the other side, which is, thus, a model of the lipid matrix of the outer membrane of Gram-negative bacteria. The concentrations of $rBPI_{21}$ in our experiments of up to 500 nM are in the range observed in the body fluids of abscess cavities harboring Gram-negative and Gram-positive bacterial species (Opal et al., 1994) or $rBPI_{23}$ peak levels after infusion with $rBPI_{23}$ (up to 10 μg/mL) (Bauer et al., 1996) but significantly higher than BPI plasma levels of healthy humans (typically less than 1 ng/mL) (Froon et al., 1995; White et al., 1994). However, due to an accumulation of $rBPI_{21}$ at negatively charged membrane surfaces the local, effective concentration of the protein at the bilayer surface is not known.

The interaction of $rBPI_{21}$ with various lipid systems results in an increase in membrane current and in a disruption of reconstituted planar membranes, provided the surface to which the protein was added was composed of negatively charged lipids (Figures 2, and 3). On the basis of the results of these studies, it is reasonable to assume that the mechanisms leading to membrane rupture involve the charge-dependent binding of $rBPI_{21}$ to the negatively charged membrane surface, its intercalation into the hydrophobic moiety, and the rigidification of the hydrocarbon chains. The influence of charges on the interaction of $rBPI_{21}$ with the bilayer membranes is further supported by the observations that (i) membrane rupture occurred at lower absolute values of the clamp voltage, when its gradient forced the polycationic $rBPI_{21}$ molecule to the membrane surface, i.e., when the clamp voltage was positive, and (ii) the increase in membrane current induced by $rBPI_{21}$ occurred in F515 LPS/

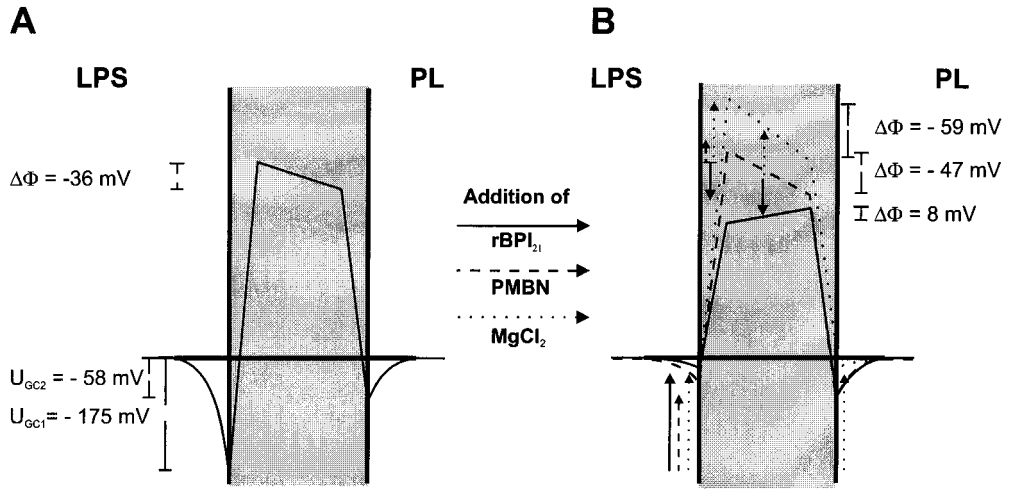

FIGURE 6: Intrinsic membrane potential profiles for F515 LPS/PL membranes in the absence (A) and in the presence of 300 nM $rBPI_{21}$ (solid line), 300 nM PMBN (dashed line), and 40 mM $MgCl_2$ (dotted line), respectively, on the LPS side of the membrane in the bathing solution (B). The Gouy-Chapman potentials were obtained from eq 1, and the trapezoidal innermembrane potential profiles were calculated from the respective fits of eq 3 to the experimental data. Changes in the height of the potential barrier were obtained from eq 2, and changes in the Gouy-Chapman potential were derived from the ζ-potential measurements (Wiese et al., 1997). The innermembrane potential differences $\Delta\Phi$ were taken from the evaluation of the corresponding *I*/*U* curve.

PL membranes at lower clamp voltages than in R45 LPS/PL membranes. From earlier measurements on the stoichiometry of $rBPI_{21}$ binding to the lipids we concluded that the rigidification may occur in distinct domains rather than homogenously over the entire membrane (Wiese et al., 1997). The borders between regions of different fluidity might serve as leaks for ion flow and as nuclei for membrane rupture.

Our findings may also explain findings of In't Veld et al. (1988), who showed that BPI disrupted the functional integrity of the cytoplasmic membrane of isolated bacterial cytoplasmic membrane vesicles of both Gram-negative and BPI-insensitive Gram-positive bacteria.

We have previously found that when the temperature of the bathing solution of LPS/PL membranes was reduced below the phase transition temperature of Re LPS, the membranes are strongly destabilized and frequently break. The destabilization caused by $rBPI_{21}$ is significantly reduced in the presence of high concentrations of $MgCl_2$, even though Mg^{2+} ions themselves may provoke a rigidification of the acyl chains and an increase in T_c of LPS aggregates (Brandenburg & Seydel, 1990). Clearly, the rigidification induced by the two agents is of different character: while Mg^{2+} ions lead to a cross-linking between the individual LPS molecules in the headgroup region, the deep intercalation of $rBPI_{21}$ into the hydrophobic moiety causes membrane disturbance and, because of the size of the protein molecules, also a spatial separation of the lipid molecules, thus reducing their intermolecular association.

The stabilizing effect of $MgCl_2$ has, furthermore, notable implications for the protection against the activity of BPI. Thus, it has been reported that 10−20 mM $MgCl_2$ protects against the permeability-increasing effects of the protein toward actinomycin D (Weiss et al., 1975, 1978, 1983, 1984). Surprisingly, $MgCl_2$ did not influence the binding of BPI to isolated LPS, whereas its binding to the surface of intact bacteria was inhibited (Weiss et al., 1975). These observations are backed by our findings that at high concentrations of $MgCl_2$ (40 mM) in the bathing solution of the membranes, the protein concentration necessary to induce an increase in membrane current was more than 10-fold higher than in the absence of $MgCl_2$. Also, $MgCl_2$ significantly reduced the influence of $rBPI_{21}$ on $\Delta\Phi$ (Figures 4B and 5). Most likely, $MgCl_2$ inhibits the incorporation of $rBPI_{21}$ into the membrane (Wiese et al., 1997).

Current fluctuations from leakages at the border between rigidified and fluid membrane areas were observed only in a few experiments with DOPG-BLMs (Figure 3B). It is obvious that the size of the corresponding lesions is too small to allow single $rBPI_{21}$ molecules to permeate. These observations are in contrast to findings from corresponding experiments with PMB, in which we showed that the decapeptide-induced transient membrane lesions are large enough to allow the passage of PMB molecules into the periplasm (Schröder et al., 1992). These differences in the action of $rBPI_{21}$ and PMB may explain the observed differences in their effects on inner membrane vesicles, although other mechanisms may also play a role (In't Veld et al., 1988).

The destabilizing effect of $rBPI_{21}$ may not represent the only mechanism operative in its lethal effect on Gram-negative bacteria. A second mechanism may be based on the influence of $rBPI_{21}$ on the intrinsic potential of the outer membrane. Due to the presence of water-filled pores formed by outer membrane proteins, differences in the ion concentrations on both sides of the outer membrane should not contribute to the transmembrane potential by charge separation. However, it was shown that gating of outer membrane proteins depends mainly on the surface potential (Wiese et al., 1994). Addition of $rBPI_{21}$ clearly led to a dramatic change in the innermembrane potential difference from $\Delta\Phi = -36$ mV for the unmodified F515 LPS/PL bilayer to +8 mV in the presence of the protein (Figure 6), as determined from the respective *I*/*U* curves (Figures 4 and 5). For R45 LPS/PL-membranes, the shift in $\Delta\Phi$ was from −37 to −5 mV. The smaller shift in the latter system may be explained by the lower surface charge density of the R45 LPS layer as compared to that of the F515 LPS layer and the therefore reduced incorporation of $rBPI_{21}$ molecules. These effects of $rBPI_{21}$ on the two membranes—one resembling the lipid matrix of the outer membrane of a PMB-sensitive (F515 LPS/

PL) species; the other, that of a PMB-resistant species (R45 LPS/PL)—are in agreement with findings that the bactericidal activity of the protein is also comparable for PMB-sensitive (*E. coli* J5) and PMB-resistant (*P. mirabilis* R45) bacteria (Capodici et al., 1994).

In contrast to the effect of $rBPI_{21}$, Mg^{2+} and PMBN caused an increase in negativity to −59 and −47 mV, respectively. These different effects of the three agents on $\Delta\Phi$ and the results of ζ-potential measurements, which gave evidence for a decrease in negativity of the surface potential on the LPS side of the membrane (Wiese et al., 1997), suggest to us that $rBPI_{21}$ (but not Mg^{2+} and PMBN) reduces the dipole potential of the LPS-leaflet. At sufficiently high concentrations Mg^{2+} can neutralize negative surface potentials (Wiese et al., 1997).

The $rBPI_{21}$-induced reduction of the dipole potential could be caused by several factors: (i) the intercalation of $rBPI_{21}$ into the membrane causes a reduction of the number of LPS molecules per unit surface, thus diminishing the contribution of the LPS molecules themselves (charge distribution in the headgroup) and the amount of bound water molecules to the dipole potential; (ii) the intercalation of $rBPI_{21}$ into the LPS leaflet leads to a reorganization of the LPS molecules (Weiss et al., 1984) and, thus, to changes in their dipole moments as well as in those of bound water molecules; and (iii) the charge distributions of the $rBPI_{21}$ molecules cause a dipole potential directed in the opposite direction to that of the LPS molecules. At present it is not possible to decide which of these factors is responsible for the observed effects.

The permeability-increasing action of BPI has been shown for actinomycin D (Weiss et al., 1978, 1983, 1984; Horwitz et al., 1995), and $rBPI_{21}$ appears to act synergistically with a number of other antibiotics (Lambert et al., 1994). The observed increase of membrane current after the addition of $rBPI_{21}$ to nonactin-doped LPS/PL membranes (Figure 4) indicates a reduction of the transmembrane potential barrier and could thus explain the higher permeability of the membrane for positively charged substances. Therefore, for an increase of membrane permeability by $rBPI_{21}$, neither the existence of water-filled pores nor the rupture of the membrane would be required.

In summary, our data show that the action of $rBPI_{21}$ on reconstituted outer membranes is mediated by electrostatic interaction of the polycationic protein with the negatively charged LPS surface, causing immobilization of the hydrocarbon chains, an increase of membrane conductivity, and eventually, membrane rupture (Wiese et al., 1997). These events may also occur in the bacterial membrane on a microscopic scale and allow $rBPI_{21}$ molecules to gain access to the cytoplasmic membrane. Furthermore, the intercalation of $rBPI_{21}$ leads to large changes in the transmembrane potential, thereby possibly influencing the gating behavior of outer membrane proteins. The reduction of the potential barrier may also explain the membrane passage of antibiotics and other molecules even in the absence of water-filled channels. All these effects can be largely suppressed by high concentrations of Mg^{2+} ions, and similar but less pronounced effects were observed with membrane systems made from negatively charged phospholipids. The demonstrated interaction of $rBPI_{21}$ with negatively charged mammalian phospholipid membranes is unlikely to be of importance *in vivo*, as Gram-negative bacteria express by far the highest negative surface charge density and, thus, the highest affinity toward BPI.

ACKNOWLEDGMENT

We are indebted to Mrs. M. Lohs for the preparation of the drawings.

REFERENCES

Bauer, R. J., White, M. L., Wedel, N., Nelson, B. J., Friedmann, N., Cohen, A., Hustinx, W. N. M., & Kung, A. H. C. (1996) *Shock 5*, 91−96.

Benz, R., & Janko, K. (1976) *Biochim. Biophys. Acta 455*, 721−738.

Brandenburg, K., & Seydel, U. (1990) *Eur. J. Biochem. 191*, 229−236.

Capodici, C., Chen, S., Sidorczyk, Z., Elsbach, P., & Weiss, J. (1994) *Infect. Immun. 62*, 259−265.

Cevc, G. (1990) *Biochim. Biophys. Acta 1031*, 311−382.

de Winter, R. J., von der Möhlen, M., van Lieshout, H., Wedel, N., Nelson, B., Friedmann, N., Delemarre, B. J. M., & van Deventer, S. J. H. (1995) *J. Inflammation 45*, 193−206.

Elsbach, P., & Weiss, J. (1993) *Immunobiology 187*, 417−429.

Elsbach, P., Weiss, J., Franson, R. C., Beckerdite-Quagliata, S., Schneider, A., & Harris, L. (1979) *J. Biol. Chem. 254*, 11000−11009.

Froon, A. H. M., Dentener, M. A., Greve, J. W. M., Ramsay, G., & Buurman, W. A. (1995) *J. Infect. Dis. 171*, 1250−1257.

Galanos, C., Lüderitz, O., & Westphal, O. (1969) *Eur. J. Biochem. 9*, 245−249.

Gazzano-Santoro, H., Parent, J. B., Grinna, L., Horwitz, A., Parsons, T., Theofan, G., Elsbach, P., Weiss, J., & Conlon, P. J. (1992) *Infect. Immun. 60*, 4754−4761.

Gazzano-Santoro, H., Parent, J. B., Conlon, P. J., Kasler, H., Tsai, C.-M., Lill-Elghanian, D. A., & Hollingsworth, R. I. (1995) *Infect. Immun. 63*, 2201−2205.

Hall, J. E., & Latorre, R. (1976) *Biophys. J. 15*, 99−103.

Hansbrough, J., Tenenhaus, M., Wikström, T., Braide, M., Rennekampff, O. H., Kiessig, V., & Bjursten, L. M. (1996) *J. Trauma 40*, 886−892.

Horwitz, A. H., Williams, R. E., & Nowakowski, G. (1995) *Infect. Immun. 63*, 522−527.

Horwitz, A. H., Leigh, S. D., Abrahamson, S., Gazzano-Santoro, H., Liu, P.-S., Williams, R. E., Carroll, S. F., & Theofan, G. (1996) *Protein Expression Purif. 8*, 28−40.

Huang, K., Fishwild, D. M., Wu, H.-M., & Dedrick, R. L. (1995) *Inflammation 19*, 389−404.

In't Veld, G., Mannion, B., Weiss, J., & Elsbach, P. (1988) *Infect. Immun. 56*, 1203−1208.

Kartalija, M., Kim, Y., White, M. L., Nau, R., Tureen, J. H., & Täuber, M. G. (1995) *J. Infect. Dis. 171*, 948−953.

Kirsch, E., Quint, P., Carroll, S., Scannon, P., Giroir, B., & BPI Study Group (1997) *Shock 7* (Suppl.), 142.

Koyama, S., Shibamoto, T., Ammons, W. S., & Saeki, Y. (1995) *Shock 4*, 74−78.

Lambert, L., Wong, P., Hoppe, P., & Scannon, P. (1994) in *Proceedings of the 35th Interscience Conference on Antimicrobial Agents and Chemotherapy*, Orlando, FL, abstr C/6, American Society for Microbiology, Washington, DC.

Latorre, R., & Hall, J. E. (1976) *Nature 254*, 361−363.

Lechner, A. J., Lamprech, K. E., Johanns, C. A., & Matuschak, G. M. (1995) *Shock 4*, 298−306.

Mannion, B. A., Weiss, J., & Elsbach, P. (1990) *J. Clin. Invest. 85*, 853−860.

McLaughlin, S. (1977) in *Current Topics in Membrane and Transport* (Bronner, F., & Kleinzeller, A., Eds.) pp 71−144, Academic Press, New York.

McLaughlin, S. (1989) *Annu. Rev. Biophys. Biophys. Chem. 18*, 113−136.

Montal, M., & Mueller, P. (1972) *Proc. Natl. Acad. Sci. U.S.A. 69*, 3561−3566.

Mueller, P., Rudin, D. O., Tien, H. T., & Wescott, W. C. (1963) *J. Phys. Chem. 67*, 534−535.

Neher, E., & Stevens, C. F. (1977) *Annu. Rev. Biophys. Bioeng. 6*, 345−381.

Ooi, C. E., Weiss, J., Elsbach, P., Frangione, B., & Mannion, B. (1987) *J. Biol. Chem. 262*, 14891−14894.

Ooi, C. E., Weiss, J., Doerfler, M. E., & Elsbach, P. (1991) *J. Exp. Med. 174*, 649−655.

Opal, S. M., Palardy, J. E., Marra, M. N., Fisher, C. J., Jr., McKelligon, B. M., & Scott, R. W. (1994) *Lancet 344*, 429−431.

Osborn, M. J., Gander, J. E., Parisi, E., & Carson, J. (1972) *J. Biol. Chem. 247*, 3962−3972.

Rietschel, E. T., Brade, H., Holst, O., Brade, L., Müller-Loennies, S., Mamat, U., Zähringer, U., Beckmann, F., Seydel, U., Brandenburg, K., Ulmer, A. J., Mattern, T., Heine, H., Schletter, J., Loppnow, H., Schönbeck, U., Flad, H.-D., Hauschildt, S., Schade, U. F., Di Padova, F., Kusumoto, S., & Schumann, R. R. (1996) in *Pathology of Septic Shock* (Rietschel, E. T., & Wagner, H., Eds.) pp 39−81, Springer-Verlag, Berlin, Heidelberg, and New York.

Schoch, P., Sargent, D. F., & Schwyzer, R. (1979) *J. Membr. Biol. 46*, 71−89.

Schröder, G., Brandenburg, K., & Seydel, U. (1992) *Biochemistry 31*, 631−638.

Seydel, U., Schröder, G., & Brandenburg, K. (1989) *J. Membr. Biol. 109*, 95−103.

Seydel, U., Eberstein, W., Schröder, G., & Brandenburg, K. (1992) *Z. Naturforsch. 47c*, 757−761.

Vinogradov, E. V., Thomas-Oates, J. E., Brade, H., & Holst, O. (1994) *J. Endotoxin Res. 1*, 199−206.

Weiss, J., & Olsson, I. (1987) *Blood 69*, 652−659.

Weiss, J., Franson, R. C., Beckerdite, S., Schmeidler, K., & Elsbach, P. (1975) *J. Clin. Invest. 55*, 33−42.

Weiss, J., Elsbach, P., Olsson, I., & Odeberg, H. (1978) *J. Biol. Chem. 253*, 2664−2672.

Weiss, J., Victor, M., & Elsbach, P. (1983) *J. Clin. Invest. 71*, 540−549.

Weiss, J., Muello, K., Victor, M., & Elsbach, P. (1984) *J. Immunol. 132*, 3109−3115.

White, M. L., Ma, J. K., Birr, C. A., Trown, P. W., & Carroll, S. F. (1994) *J. Immunol. Methods 167*, 227−235.

Wiese, A., Schröder, G., Brandenburg, K., Hirsch, A., Welte, W., & Seydel, U. (1994) *Biochim. Biophys. Acta 1190*, 231−242.

Wiese, A., Brandenburg, K., Lindner, B., Schromm, A. B., Carroll, S. F., Rietschel, E. T., & Seydel, U. (1997) *Biochemistry 36*, 10301−10310.

BI970177E